Legal Medicine 76 (2025) 102635

Contents lists available at ScienceDirect

Legal Medicine

journal homepage: www.elsevier.com/locate/legalmed

NF-κB and SIRT1 evaluation to discriminate antemortem from postmortem wounds. Potential markers of skin wound vitality in forensic practice

Gabriella Teti [a], Filippo Pirani [b,*], Simone Gavelli [b], Alberto Gualandi [c], Maria Carla Mazzotti [d], Luca Berti [b], Mirella Falconi [e], Susi Pelotti [b], Paolo Fais [b]

[a] Department of Biomedical and Neuromotor Sciences, University of Bologna 40126 Bologna, Italy
[b] Department of Medical and Surgical Sciences, Unit of Legal Medicine, University of Bologna 40126, Italy
[c] Institute of Pathology, DAME, University Hospital of Udine 33100 Udine, Italy
[d] Polizia di Stato, Department of Public Security, Ministry of Interior, Italy
[e] Department of Medical and Surgical Sciences, University of Bologna, 40126, Italy

ARTICLE INFO

Keywords:
Forensic pathology
Wound vitality
NF-κB
SIRT1
Immunohistochemistry
Western blot

ABSTRACT

Background many studies have been conducted on wound age estimation, but to date no marker has been validated to use in routine forensic practice. To explore novel markers for vitality of wounds, we investigated the expression of the inflammatory-related marker nuclear factor kappa B (NF-κB) and analyzed its correlation with the silent information regulator sirtuin 1 (SIRT1) protein in skin wounds. Methods: on 8 amputated human limbs we collected human skin tissue samples from the amputation site, as antemortem samples, and from wounds produced on the stored corresponding limbs, as postmortem samples. Samples were processed for western blot and immunohistochemistry analysis to evaluate the ex-pression of NF-κB and SIRT1 proteins. Results: cytoplasmic and nuclear staining of NF-κB in epidermal cells of antemortem wounds was higher than in postmortem wounds, where the NF-κB signal was mainly localized in the nuclei of keratinocytes. Quantitative analysis demonstrated a 2-fold increase in NF-κB protein in antemortem wounds. On the contrary, SIRT-1 levels were almost absent in antemortem wounds, while high nuclear staining was detected in keratinocytes in postmortem wounds. Quantitative analysis of the stained area demonstrated a 3-fold increase in SIRT1 protein in postmortem wounds. Conclusions: analysis of NF-κB and SIRT1 showed a different qualitative and quantitative pattern of expression in antemortem and postmortem wounds. They represent good candidates as biomarkers in wound vitality estimation in forensic pathology eventually to include them in a panel of biomarkers.

1. Introduction

Demonstrating whether a wound was produced antemortem or postmortem is crucial in forensic pathology, especially for skin wounds, as it can influence the judicial reconstruction of events. However, determining wound vitality poses a complex challenge for forensic pathologists, as it requires analysing multiple data, including circumstantial data, and both macroscopic and microscopic findings, to assess the biochemical and cell- mediated events that occur in altered tissues to restore functional and structural integrity [1]. To evaluate wound vitality, morphological, cytological, biochemical, histological, and immunohistochemical techniques can be used, each capable of capturing and highlighting some of the typical aspects of this succession of events (such as haemorrhage, acute inflammation, proliferation, and tissue remodelling) [2,3]. The main histological findings for wound vitality evaluation are red blood cells infiltration, inflammatory reactions, presence of fibroblasts, macrophages, and immigrating granulocytes, as well as tissue alterations [2,4]. However, these features may not be present at all or may occur even after death, so standard histological examination alone may not always determine whether the wound was inflicted antemortem or postmortem [4,5]. Recent studies have focused on identifying relevant markers of vital origin using immunohistochemical techniques, but to date, no single marker has proven efficient and reliable, although some appear promising [4]. The most common immunostainings highlight the presence of molecules linked to tissue damage in the injured tissues, exploiting the interaction between an

* Corresponding author.
E-mail addresses: gabriella.teti2@unibo.it (G. Teti), filippo.pirani2@unibo.it (F. Pirani), a.gualandi@icloud.com (A. Gualandi), mariacarla.mazzotti@poliziadistato.it (M.C. Mazzotti), mirella.falconi@unibo.it (M. Falconi), susi.pelotti@unibo.it (S. Pelotti), paolo.fais@unibo.it (P. Fais).

https://doi.org/10.1016/j.legalmed.2025.102635
Received 20 January 2025; Received in revised form 7 May 2025; Accepted 21 May 2025
Available online 23 May 2025

antibody and a specific antigen of interest.

The inflammatory-related marker nuclear factor kappa B (NF-κB) and the silent information regulator sirtuin 1 (SIRT1) are transcription factors that act within the cell nucleus in damaged tissues. Specifically, SIRT1 has been observed to inhibit the expression of factors involved in different pro-inflammatory pathways, such as HIF1α and activating protein 1 (AP-1) [6]. In contrast, NF-κB plays an opposite role during the inflammatory response, stimulating the expression of many pro-inflammatory cytokines, such as IL-1β, IL-6, TNF-α, and CCL2 [7].

Given the pivotal role of these markers in modulating the inflammatory response in tissue damage, the objective of this study is to assess the expression of SIRT1 and NF-κB in vital and non-vital skin wounds on amputated limbs using western blotting and immunohistochemical techniques.

2. Materials and methods

2.1. Sample collection

Antemortem injuries were considered fragments of skin tissues (1–1.5 cm^2) were collected at the site of amputation from 8 lower limbs of patients (n = 8) that underwent surgery for traumatic or natural conditions. The limbs belonged to 5 men and 3 women with age ranging from 54 to 79 years (Table 1). The limbs were stored at 4 °C and post-mortem skin wounds (1–1.5 cm^2) were collected with a scalpel in the corresponding limb of the ante-mortem wound, far from the site of amputation.

Skin samples were taken between 12 and 24 h after surgery. The study was carried according to the guidelines of the Bioethics Committee of the University of Bologna, which approved the research project according to protocol n°75975 of 26/03/2021.

2.2. Protein extraction and western blot

After collection skin samples were stored at −80 °C until protein extraction. RIPA modified lysis buffer (Pierce, Thermo Fisher Scientific, Monza, Italy) supplemented with 25 μmol/L protease inhibitor cocktail (Pierce, Thermo Fisher Scientific, Monza, Italy) and 1 μL of β-mercaptoethanol (Sigma-Aldrich, St. Louis, Missouri, USA) was used for total protein extraction. Bradford assay (Sigma-Aldrich, St. Louis, Missouri, USA) was performed to quantify the amount of total protein obtained from each sample. 4–12 % sodium dodecyl sulfate polyacrylamide gel electrophoresis (SDS-PAGE) was utilized to separate 15 μg of total protein which were subsequently transferred onto a nitrocellulose membrane (GE Healthcare, Amersham, UK) using a transfer wet system. Then, the membranes were incubated with 5 % bovine serum albumin (BSA) (blocking reagent) to reduce the non-specific binding background, followed by incubation with the primary antibodies against rabbit anti-NF-κB antibody (Cell Signaling Technologies, Euroclone, Milan, Italy), rabbit anti-SIRT1 antibody (Cell Signaling Technologies, Euroclone, Milan, Italy) and anti-tubulin antibody (Millipore Merck, Darmstadt, Germany). All the primary antibodies were diluted 1:1000 in blocking reagent at 4 °C, overnight. Three washes with TBS-tween buffer were performed to eliminate the unreacted primary antibodies. Then, the membranes were incubated with HRP-linked anti-rabbit or anti-mouse IgG secondary anti-bodies, diluted 1:2000 in TBS-tween buffer (Sigma Aldrich, St Louis, Missouri, USA). The enhancement chemiluminescence system (Pierce, Thermo Fisher Scientific, Monza, Italy) was used to detect the antibody signal. Images were obtained by using IBright Western Blot Imaging System (Thermo Fisher Scientific, Monza, Italy). Image J software (National Institutes of Health, USA) was utilized for the densitometric analysis. The intensities of the specific protein bands were corrected for equal tubulin loading and they were expressed as relative value compared to the intensity of the respective control sample. Data showed the average of triplicates ± SD.

Table 1

Sample	Age	Gender	Comorbidities	Cause leading to amputation
1	54	F	None	Lower limb trauma
2	76	M	Hypertension and diabetes	Lower limb ulcers
3	75	F	Hypertension and diabetes	Lower limb ulcers
4	79	M	Hypertension and diabetes	Lower limb ulcers
5	72	M	Hypertension and diabetes	Lower limb ulcers
6	75	F	Hypertension and diabetes	Lower limb ulcers
7	76	M	Hypertension and diabetes	Lower limb ulcers
8	62	M	None	Lower limb trauma

2.3. Sample processing for light microscopy analysis

4 % formaldehyde (Sigma Aldrich, St Louis, MO, USA) in phosphate-buffered saline (PBS) was used to fix skin tissues samples immediately after collection. All the samples were fixed for 24 h, at 4 °C. After three washes in PBS and distilled water, the samples were dehydrated in a graded series of ethanol solutions and embedded in paraffin wax (Fluka, Sigma-Aldrich). An automated rotary microtome (Leica Microsystems Srl, Cambridge, UK) was utilized to obtain paraffin sections of 5 μm which were collected on Superfrost glass slides (Carl Roth, Karlshure, Germany) and let them dried until staining proce-dures.

2.4. Goldner's Masson trichrome staining

Paraffin embedded skin sections were dewaxed and then washed three times in distilled water. Then, samples were stained by Goldner's Masson trichrome staining procedure according to manufacturer instructions (Bio-optica, Milan, Italy). Samples were subsequently ethanol dehydrated, mounted with resinous mounting medium and observed under a light microscope using an Eclipse E800 Nikon (Nikon, Tokyo, Japan).

2.5. Immunohistochemistry

Paraffin tissue sections were dewaxed and rehydrated in graded series of ethanol solutions. At the end of the hydration process, the sections were washed three times for 5 min with PBS at pH 7.4. 10 mM sodium citrate in PBS was utilized for the antigen retrieval procedure. Samples were left in the sodium citrate solution for 30 min at 60 °C. Endogenous peroxidase activity was blocked with 3 % H2O2 (diluted in distilled water) at room temperature (RT) for 15 min. Protein block milk (Invitrogen, Thermo Fischer Scientific, Monza, Italy) was used to block the non-specific antibody binding. Samples were left for 30 min at RT. Then, the sections were incubated with the primary antibody anti-human NF-κB p65 (Cell signaling, Massachusetts, USA), diluted 1:400 or anti-human SIRT1 (Cell signaling, Massachusetts, USA) diluted 1:200 in blocking solution at 4 °C overnight. At the end of the incubation, samples were washed three times in PBS and incubated with the secondary anti-rabbit antibody for 30 min at RT followed by diaminobenzidine tetrahydrochloride (DAB) as substrate staining solution (Histofine Immunohistochemical staining kit, Nichirei Biosciences, Tokyo, Japan). Negative controls consisted in samples in which the primary antibodies and/or the secondary antibody was omitted followed by DAB staining. All samples were observed under a light microscope using an Eclipse E800 Nikon (Nikon, Tokyo, Japan). Representative images are shown. The quantitative analysis of antibody-stained areas was assessed by area counting of five fields for each of three slides per sample at 60 × magnification by the Leica Qwin 3.0 software (Leica Microsystems Srl, Cambridge, UK).

2.6. Transmission electron microscopy (TEM)

A solution of 2.5 % (v/v) glutaraldehyde in 0.1 M cacodylate buffer was used to fix skin samples just after their collection. The fixation step was performed for 2 h at 4 °C followed by a post fixation step consisting in letting samples in a solution of 1 % (w/v) osmium tetroxide in 0.1 M cacodylate buffer for 30 min at RT. After some washes in 0.15 M cacodylate buffer, samples were dehydrated by a graded series of acetone solutions and finally embedded in epoxy resin (Fluka, Sigma-Aldrich). The embedded samples were cut into ultrathin slices (100 nm thickness), stained by uranyl acetate solution and lead citrate, and then observed by transmission electron microscope CM10 Philips (FEI Company, Eindhoven, The Netherlands) at an accelerating voltage of 80 kV. Images were recorded by Megaview III digital camera (FEI Company, Eindhoven, The Netherlands).

2.7. Statistical analysis

Prism 6 (GraphPad San Diego, CA, USA) was used to perform all statistics. Student's *t*-test was applied between each antemortem injury and the respective control sample for each patient. The differences were considered significant at $p < 0.05$.

3. Results

3.1. Morphological analysis by Goldner's Masson trichrome staining

Light microscopy analysis by Goldner's Masson trichrome staining of skin tissues showed a preserved morphology in all the skin compartments, in both antemortem and postmortem samples (Fig. 1A and 1C). No significant morphological changes in epidermis and dermis and no aggregation of inflammatory cells were detected in antemortem (Fig. 1A and 1B) and postmortem injuries (Fig. 1C and 1D) connected to a vital reaction in antemortem wounds.

3.2. NF-κB and SIRT1 protein expression by western blot analysis

No significant difference in the expression of NF-κB protein was observed in antemortem wounds compared to the postmortem control samples (Fig. 2A and 2B). On the contrary, a significant difference in the expression of SIRT1 protein was evaluated in all antemortem samples compared postmortem samples of the same limb (Fig. 2C). Densitometric analysis of protein bands demonstrated a light down-regulation of the SIRT1 protein at almost all antemortem samples tested in the study (Fig. 2D).

3.3. Immunohistochemical detection of NF-κB protein in skin wounds sections

Immunohistochemical sections of ante-mortem skin tissues showed a weak signal of NF-κB protein, mainly localized in epidermis (Fig. 3A). A low level of protein expression was also detected in dermis, endothelial cells of blood vessel and ductal cells of sweat glands. At higher magnification, almost all the keratinocytes of the different layers of the epidermis showed a weak but widespread signal of the NF-κB protein in both cytoplasm and nucleus (Fig. 3B).

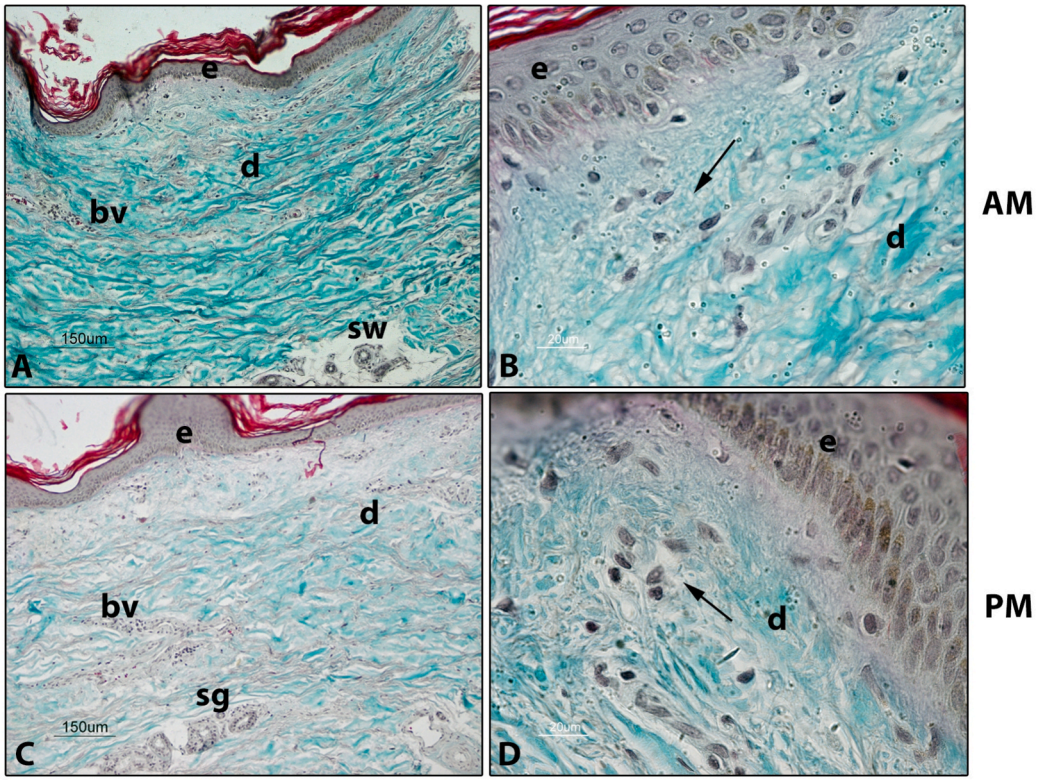

Fig. 1. Goldner's Masson trichrome staining of representative images of antemortem (AM) and postmortem (PM) wound sections. (A) antemortem wounds in which epidermis (e) and dermis (d) are well detected. In the dermis blood vessel (bv) sweat glands (sg) are observed (magnification 10X; bar: 150 mm). (B) high magnification image of antemortem wounds. The different layers of the epidermis (e) are well detected. The green color observed in the dermis (d) indicates a wide distribution of collagen fibers. Several nuclei of dermal cells are detected (arrow). No aggregation of inflammatory cells is identified in the dermis (magnification 60X; bar: 20 mm). (C) postmortem wounds in which epidermis (e) and dermis (d) are well observed. In the dermis, blood vessels (bv) and sweat glands (sg) are easily identified (magnification 10X; bar: 150 mm). (D) high magnification image of postmortem wounds. The different layers of the epidermis (e) and the collagen components of the dermis are well detected. Several nuclei of dermal cells are detected (arrow) (magnification 60X; bar: 20 mm). Sample n. 1. (For interpretation of the references to color in this figure legend, the reader is referred to the web version of this article.)

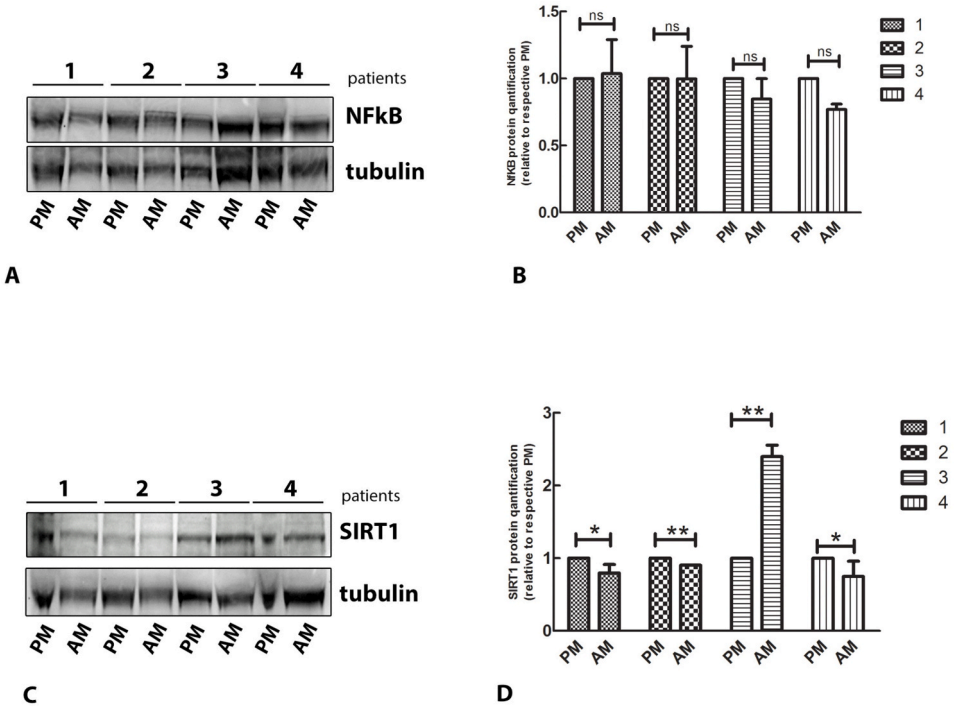

Fig. 2. (A) representative western blot images showing the expression of the protein NF-κB in antemortem (AM) and postmortem (PM) skin injuries (n = 4). (B) Relative amount of NF-κB protein expression normalized to the intensity of tubulin protein and represented as fold changes relative to each respective PM. Western blot was performed in duplicate, and the relative quantification is expressed as mean value ± SD. (C) representative western blot images showing the expression of the protein SIRT1 in antemortem (AM) and postmortem (PM) skin injuries (n = 4). (D) Relative amount of SIRT1 protein expression normalized to the intensity of tubulin protein and represented as fold changes relative to each respective PM. Western blot was performed in duplicate, and the relative quantification is expressed as mean value ± SD. * $p < 0.05$; ** $p < 0.001$.

Immunohistochemical postmortem skin sections, showed a stronger NF-κB protein signal compared to antemortem sections, mainly localized in the epidermis (Fig. 3D). In dermis, endothelial cells of blood vessels and ductal cells of sweat glands also demonstrated an intense sign of the protein. At higher magnification, a specific localization of the NF-κB protein is observed in several nuclei of the epidermal keratinocytes (Fig. 3E). Quantitative analysis showed an increase of almost 1.5-fold of NF-κB stained areas in antemortem specimens compared to postmortem skin sections (Fig. 3G).

3.4. Immunohistochemical detection of SIRT1 protein in skin wounds sections

Immunohistochemical skin sections of antemortem injuries showed a weak signal of SIRT1 protein, in both epidermis and dermis (Fig. 4A). At higher magnification a low level of the protein is detected in few nuclei of the epidermis (Fig. 4B), while no sign of the protein is observed in any cellular components of the dermis.

On the contrary, postmortem sections of skin wounds showed a dark signal of the SIRT1 protein, mainly localized in the epidermis (Fig. 4 D). High magnification images showed several nuclei of the different layers of the epidermis characterized by a deep brown color corresponding to the SIRT1 protein (Fig. 4E). A 0.5 fold decrease of SIRT1 stained areas in antemortem skin sections was observed compared to postmortem sections (Fig. 4G).

3.5. Ultrastructural analysis of antemortem and postmortem skin wounds

In order to better detect any ultrastructural morphological change correlated to vital wounds, TEM analysis was carried out on antemortem and postmortem skin wounds. Results showed well preserved morphology in epidermis and dermis of antemortem skin tissues (Fig. 5A). At higher magnification, keratinocytes characterized by the presence of several melanin granules are easily detectable (Fig. 5B and 5C). Nuclei are well preserved while a few mitochondria with collapsed internal cristae are observed (Fig. 5C).

TEM analysis of postmortem skin sections showed well preserved morphology in both epidermis and dermis (Fig. 5D). Images at higher magnification showed keratinocytes characterized by several mitochondria, fibrillar keratin proteins and a reduced number of melanin granules (Fig. 5E). The cytoplasm is almost entirely filled by several mitochondria with internal cristae well detected (Fig. 5F).

4. Discussion

Many studies have been conducted concerning wound age estimation, but to date no marker has been validated to use in routine forensic practice [2–5]. Based on their roles in processes involved in *peri*-mortem cell signalling, NF-κB and SIRT1 were evaluated to formulate a differential diagnosis between antemortem and postmortem skin wounds.

NF-κB and SIRT1 are produced within the cell at the cytoplasmic level. Subsequently, they translocate inside the nucleus to express their function as transcription factors, modulating the inflammatory response and many other cellular biological pro-cesses. SIRT1 acts as a repressor of the inflammatory response, suppressing the expression of numerous molecules involved in inflammation and wound healing processes, including IL1 [6]. It also mediates the cellular response to ischemic insults and is active during autolytic and autophagic processes [8,9]. NF-κB acts as a trigger of the activation of the inflammatory cascade, directly stimulating the production of numerous pro-inflammatory cytokines [10].

In the proposed model, the amputation margin represents the antemortem wound, while the postmortem wound was produced experimentally on the skin of the limb, far from the amputation point a few hours after the amputation, when circulation had ceased, and the vital reaction was absent or extremely weak. When death occurs, the

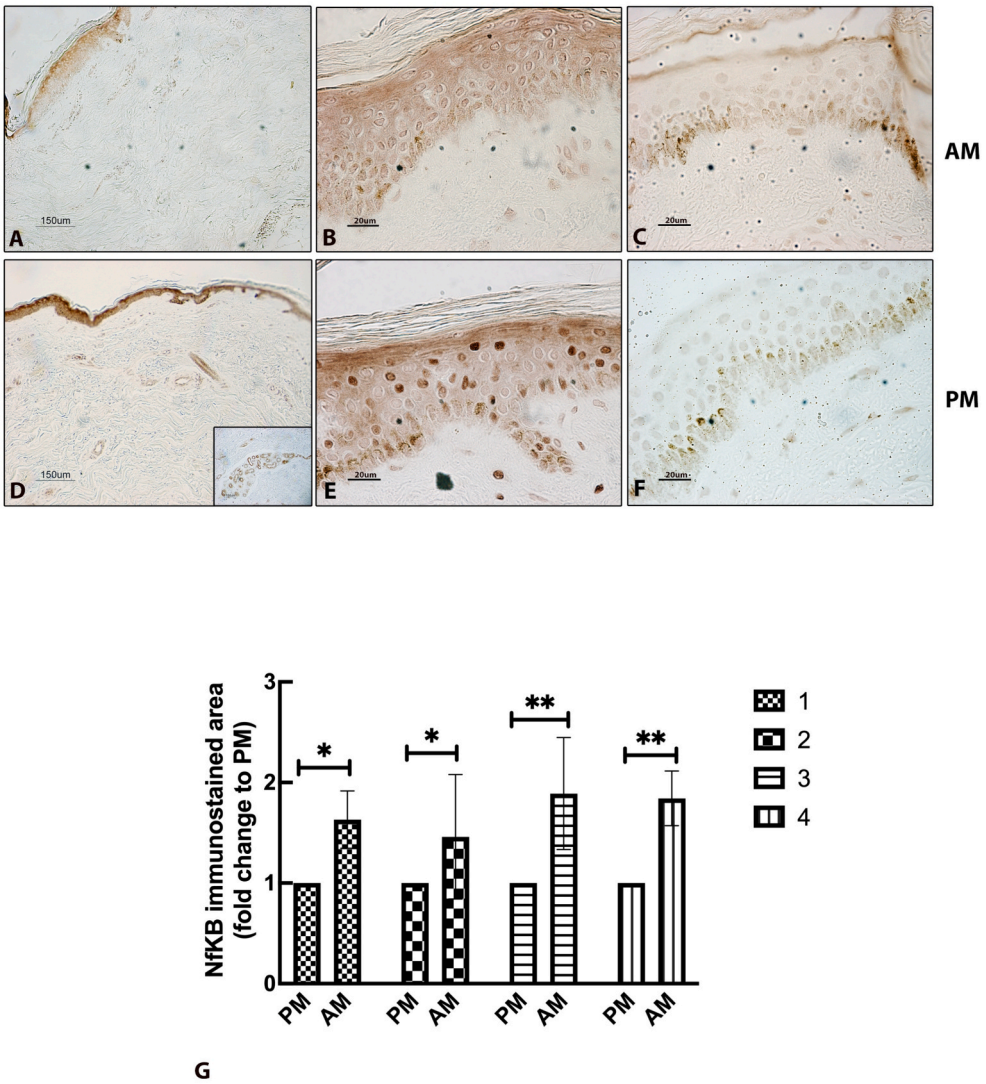

Fig. 3. Representative images of antemortem and postmortem skin wound sections immunostained to detect NF-κB protein. (A) low magnification images of antemortem skin wounds. A weak signal of the protein is mainly detectable in the epidermis (bar: 150 mm). (B) Detail of the epidermis in which the different layers of keratinocytes are easily detected. A weak signal of the NF-κB protein is widespread in almost all the cells of the epidermis (bar: 20 mm); (C) negative control images in which the primary anti-NF-κB antibody was omitted (bar: 20 mm); (D) postmortem skin wounds sections showing a strong signal of the NF-κB protein mainly localized in the epidermis. In the dermis, endothelial and sweat cells showed a positive signal (insert) (bar: 150 mm); (E) A weak signal of the protein is easily detected in all the keratinocytes of the epidermis. Several nuclei spread in the different layers of the epidermis, showed a deep signal (bar: 20 mm); (F) negative control images in which the primary anti-NF-κB antibody was omitted (bar: 20 mm). Sample n. 1.

molecular and enzymatic patterns within the cell are delayed and not altered by postmortem phenomena if autolysis is kept at bay by refrigeration. The detection of specific immunohistochemical patterns in the tissue should therefore be an expression of the molecular and enzymatic phenomena that occur in vital wounds [11]. Protein analysis was performed by western blot, densitometric, and immunohistochemical methods to evaluate the different protein expression in antemortem and postmortem wound samples both quantitatively and qualitatively.

No statistically significant differences in quantitative protein expression of NF-κB were found between antemortem and postmortem wound specimens, as determined by western blot and densitometric analysis. However, immunohistochemical investigation revealed that NF-κB was widely distributed, both at the nuclear and cytoplasmic levels, in vital wounds. In contrast, in postmortem wounds, NF-κB was more concentrated in the nuclear territory, with less cytosolic positivity. The production of NF-κB is increased in response to inflammatory stimuli, particularly in the cytoplasm [12]. This, combined with the process of cellular post-mortal autolysis, could explain the differences in marker distribution between antemortem and postmortem wound samples. Indeed, immunohistochemical analysis indicated that the cytoplasm of cells from vital wounds had a significantly higher level of NF-κB due to increased cytosolic production in response to inflammatory stimuli. Conversely, the cytoplasm of cells near non-vital wounds showed lower levels of NF-κB, possibly due to the absence of cytosolic inflammatory production along with the activity of lytic enzymes that can degrade proteic molecules, including NF-κB, before they perform their function. These findings suggest that vital wounds may exhibit more intense NF-κB activity than non-vital wounds, since an intense inflammatory response triggered by NF-κB activation is established in vital wounds.

About SIRT1, a slight but statistically significant decrease in expression was observed in antemortem wounds compared to postmortem wounds, as determined by Western blot and densitometric analysis. Immunohistochemical analysis of all samples yielded similar results. Samples taken postmortem from non-vital wounds are characterized by strong ischemic suffering, oxidative stress, and intense

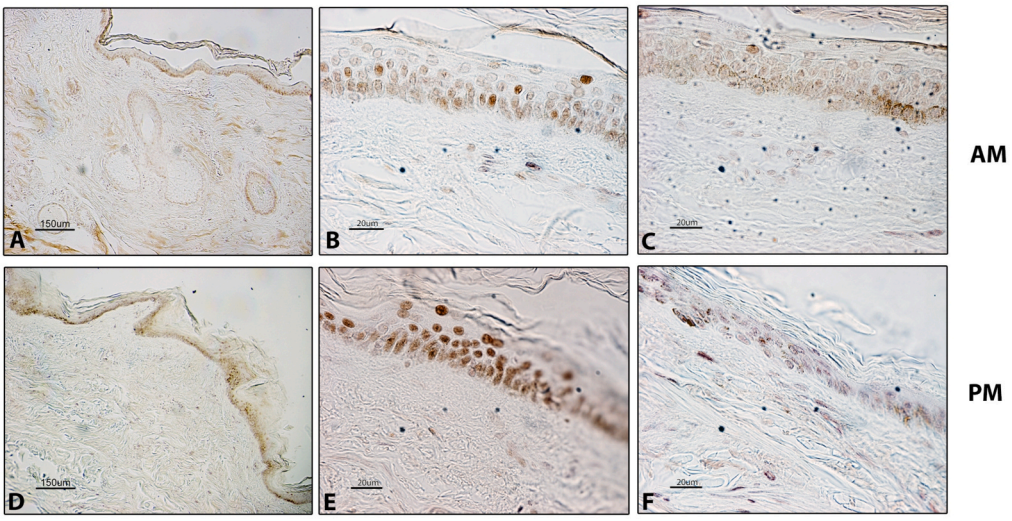

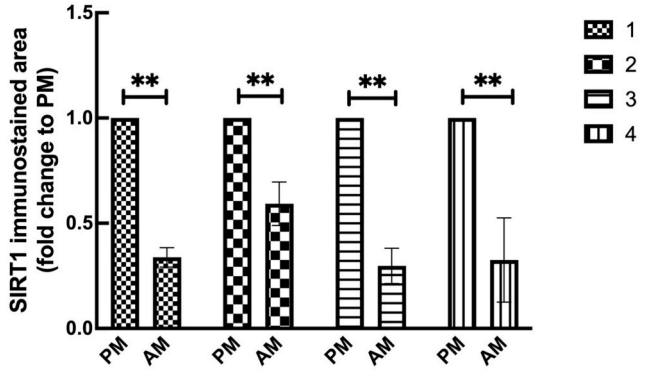

G

Fig. 4. Representative images of antemortem and postmortem skin wound sections immunostained to detect SIRT1 protein. (A) low magnification images of antemortem skin wounds. Almost no sign of the protein is detected in epidermis and dermis (bar: 150 mm). (B) Detail of the epidermis in which the different layers of keratinocytes are easily detected. A weak signal of the SIRT1 protein is observed in a few nuclei (bar: 20 mm); (C) negative control images in which the primary anti-SIRT1 antibody is omitted (bar: 20 mm); (D) postmortem skin wounds sections showing a strong signal of the SIRT1 protein mainly localized in the epidermis. (E) Several nuclei of the epidermis show a deep brown signal corresponding to SIRT1 protein (bar: 20 mm); (F) negative control images in which the primary anti-SIRT1 antibody is omitted (bar: 20 mm). Sample n. 4.

autolytic activity, in the absence of NF-κB-mediated inflammatory activation [13,14]. The greater activation of SIRT1 in non-vital wounds is partly justified, considering its role as a mediator of cellular response to ischemic suffering, activation of autolytic and autophagic processes, and response to the production of free radicals [8,15–17]. The bidirectional regulatory interaction between SIRT1 and NF-κB may instead explain the reduced presence of SIRT1 in vital wounds. On one hand, SIRT1 inhibits the binding of NF-κB to DNA, while on the other hand, the promoter of SIRT1 possesses binding sites for NF-κB, suggesting that NF-κB may itself be able to inhibit the expression of SIRT1 [18–21]. Since NF-κB is a proinflammatory factor, its activation is greater than that of SIRT1 in the context of vital wounds, thus it is possible to hypothesize that the low presence of SIRT1 in vital skin wounds is also related to a regulatory imbalance between SIRT1 and NF-κB, in favour of the latter. These considerations explain the lower expression of SIRT1 in antemortem wounds compared to postmortem ones.

In order to demonstrate the presence of autolytic processes in skin samples, an ultrastructural analysis by TEM was carried out with the aim to observe morphological changes and/or cellular organelles correlated with the autolytic reactions. The results clearly showed a light chromatin condensation in nuclear keratinocytes while no cell shrinking, intracytoplasmic vacuolization and the occurrence of lysosomes, indicators for autolysis [22] were observed. On the contrary, a great number of swelling and collapsed mitochondria were detected although they are considered by the scientific literature as unreliable markers of autolysis [22]. Keratinocytes are responsible of a high balanced process of differentiation until cornification to support the function of protective barrier of the skin. To this aim programmed cell death in the form of apoptosis is essential for maintaining and restoring skin homeostasis. Apoptosis is a not lytic cell death and typically it is not a inflammatory process [23]. The body of evidence supports the idea that reduced expression of NF-κB pathway allows spontaneous keratinocytes apoptosis to occur (i.e. postmortem samples). On the other hand, acute inflammation is a healthy response to danger signal such as trauma (i.e. antemortem samples) which activate inflammatory transcription via NF-κB [23].

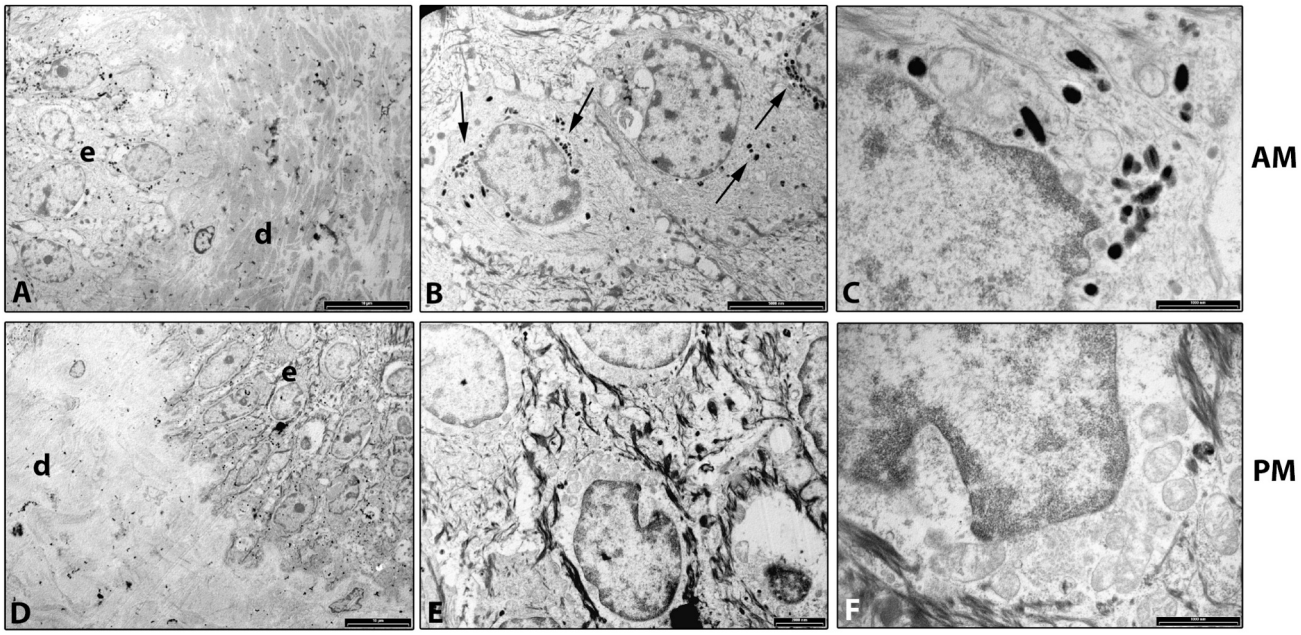

Fig. 5. TEM representative images of ultrastructural morphological analysis of antemortem and postmortem skin wounds. (A) antemortem skin wounds in which epidermis (e) and dermis (d) are easily detected (bar: 10 mm); (B) Keratinocytes in the epidermis of antemortem skin wounds. Nuclei and cytoplasm are well preserved and detected. Several melanin granules are observed (arrow) (bar: 5000 nm); (C) Detail of keratinocyte cytoplasm showing melanin granules and a few mitochondria with the internal cristae almost collapsed (bar: 500 nm); (D) postmortem skin wounds in which epidermis (e) and dermis (d) are easily detected (bar: 10 mm); (E) Keratinocytes in which several mitochondria (m) and keratin filamentous proteins (arrow) are detected. A few melanin granules are observed (bar: 2000 nm); (F) several mitochondria with preserved cristae are detected (bar: 1000 nm). Sample n. 2.

A limitation of this study is the small number of cases considered. Moreover, although SIRT1 and NF-κB have never been analyzed in forensics, they are multifunctional molecules that act on numerous signaling pathways, making it complex to interpret their behavioral and activation patterns. The potential influence of factors such pathologies affecting limb, age and gender and on the expression of SIRT1 and NF-κB was not investigated in this study. Finally, the study does not include a time-course analysis to track the degradation or persistence of SIRT1 and NF-κB expression postmortem.

Even if more studies are needed, our results showed that NF-κB and SIRT1 could be potential valuable biomarkers for wound vitality estimation in forensic practice. Future studies should focus on the validation and their inclusion in a panel of markers usefull to the development of more reliable and objective methods for determining wound vitality in forensic investigations.

Declaration of competing interest

The authors declare that they have no known competing financial interests or personal relationships that could have appeared to influence the work reported in this paper.

Acknowledgement

None.

References

[1] L.C. Borish, J.W. Steinke, Cytokines and chemokines, *J. Allergy Clin. Immunol.* 111 (2 Suppl) (2003) S460–S475, https://doi.org/10.1067/mai.2003.108.
[2] Dettmeyer RB. Vitality, Injury age, determination of skin wound age, and fracture age. In forensic histopathology, 1st Ed, Dettmeyer RB. Ed, Springer-Verlag Berlin Heidelberg, 2011, pp. 191-209 DOI 10.1007/978-3-642-20659-7_10.
[3] G. Pennisi, M. Torrisi, G. Cocimano, M. Esposito, M. Salerno, F. Sessa, Vitality markers in forensic investigations: a literature review, *Forensic Sci. Med. Pathol.*. 19 (1) (2023 Mar) 103–116, https://doi.org/10.1007/s12024-022-00551-9.
[4] J.M. Casse, L. Martrille, J.M. Vignaud, G. Gauchotte, Skin wounds vitality markers in forensic pathology: an updated review, *Med. Sci. Law* 56 (2) (2016) 128–137, https://doi.org/10.1177/0025802415590175.
[5] A. Maiese, A.C. Manetti, N. Iacoponi, E. Mezzetti, E. Turillazzi, M. Di Paolo, R. La Russa, P. Frati, V. Fineschi, State-of-the-art on wound vitality evaluation: a systematic review, *Int. J. Mol. Sci.* 23 (13) (2022) 6881, https://doi.org/10.3390/ijms23136881.
[6] J.W. Hwang, H. Yao, S. Caito, I.K. Sundar, I. Rahman, Redox regulation of SIRT1 in inflammation and cellular senescence, *Free Radic. Biol. Med.* 61 (2013) 95–110, https://doi.org/10.1016/j.freeradbiomed.2013.03.015.
[7] B.C. Albensi, What is nuclear factor kappa B (NF-κB) doing in and to the mitochondrion? *Front. Cell Dev. Biol.*. 7 (7) (2019) 154, https://doi.org/10.3389/fcell.2019.00154.
[8] U. Bond, M.J. Schlesinger, Ubiquitin is a heat shock protein in chicken embryo fibroblasts, *Mol. Cell Biol.*. 5 (5) (1985) 949–956, https://doi.org/10.1128/mcb.5.5.949-956.1985.
[9] K. Shimizu, S. Ohtani, H. Shiono, T. Fukusima, M. Sasaki, Expression of ubiquitin protein in each organ at death from hypothermia, *Forensic Sci. Int.*. 86 (1–2) (1997 18) 61–68, https://doi.org/10.1016/s0379-0738(97)02117-8.
[10] S.C. Sun, S.C. Ley, New insights into NF-kappaB regulation and function, *Trends Immunol.*. 29 (10) (2008) 469–478, https://doi.org/10.1016/j.it.2008.07.003.
[11] P. Saukko, The Pathology of Wounds. In Knight's Forensic Pathology, 4th Ed, Saukko P., Knight B. Eds, CRC Press London, 2016, pp. 133–166.
[12] P. Pai, S. Sukumar, HOX genes and the NF-κB pathway: a convergence of developmental biology, inflammation and cancer biology, *Biochim. Biophys. Acta.* 1874 (2) (2020) 188450, https://doi.org/10.1016/j.bbcan.2020.188450.
[13] J. Yang, J. Qi, B. Xiu, B. Yang, C. Niu, H. Yang, Reactive oxygen species play a biphasic role in brain ischemia, *J. Invest. Surg.*. 32 (2) (2019) 97–102, https://doi.org/10.1080/08941939.2017.1376131.
[14] P.E. Hasuoka, J.P. Iglesias, M. Teves, M.M. Kaplan, N.H. Ferrúa, P.H. Pacheco, Selenomethionine administration decreases the oxidative stress induced by post mortem ischemia in the heart, liver and kidneys of rats, *Biometals*. 34 (4) (2021) 831–840, https://doi.org/10.1007/s10534-021-00310-3.
[15] X. Meng, J. Tan, M. Li, S. Song, Y. Miao, Q. Zhang, Sirt1: role under the condition of ischemia/hypoxia, *Cell. Mol. Neurobiol.*. 37 (1) (2017) 17–28, https://doi.org/10.1007/s10571-016-0355-2.
[16] Y.S. Hori, A. Kuno, R. Hosoda, M. Tanno, T. Miura, K. Shimamoto, Y. Horio, Resveratrol ameliorates muscular pathology in the dystrophic mdx mouse, a model for Duchenne muscular dystrophy, *J. Pharmacol. Exp. Ther.*. 338 (3) (2011) 784–794, https://doi.org/10.1124/jpet.111.183210.
[17] C. Xu, L. Wang, P. Fozouni, G. Evjen, V. Chandra, J. Jiang, C. Lu, M. Nicastri, C. Bretz, J.D. Winkler, R. Amaravadi, B.A. Garcia, P.D. Adams, M. Ott, W. Tong, T. Johansen, Z. Dou, S.L. Berger, SIRT1 is downregulated by autophagy in senescence and ageing, *Nat. Cell Biol.*. 22 (10) (2020) 1170–1179, https://doi.org/10.1038/s41556-020-00579-5.

[18] F. Yeung, J.E. Hoberg, C.S. Ramsey, M.D. Keller, D.R. Jones, R.A. Frye, M.W. Mayo, Modulation of NF-kappaB-dependent transcription and cell survival by the SIRT1 deacetylase, *EMBO J.* 23 (12) (2004) 2369–2380, https://doi.org/10.1038/sj.emboj.7600244.

[19] P. Kong, Y. Yu, L. Wang, Y.Q. Dou, X.H. Zhang, Y. Cui, H.Y. Wang, Y.T. Yong, Y. B. Liu, H.J. Hu, W. Cui, S.G. Sun, B.H. Li, F. Zhang, M. Han, circ-Sirt1 controls NF-κB activation via sequence-specific interaction and enhancement of SIRT1 expression by binding to miR-132/212 in vascular smooth muscle cells, *Nucleic Acids Res.* 47 (7) (2019) 3580–3593, https://doi.org/10.1093/nar/gkz141.

[20] D. Khadka, H.J. Kim, G.S. Oh, A. Shen, S. Lee, S.B. Lee, S. Sharma, S.Y. Kim, A. Pandit, S.K. Choe, T.H. Kwak, S.H. Yang, H. Sim, G.H. Eom, R. Park, H.S. So, Augmentation of NAD^+ levels by enzymatic action of NAD(P)H quinone oxidoreductase 1 attenuates adriamycin-induced cardiac dysfunction in mice, *J. Mol. Cell. Cardiol.*. 124 (2018) 45–57, https://doi.org/10.1016/j.yjmcc.2018.10.001.

[21] N. Braidy, G.J. Guillemin, H. Mansour, T. Chan-Ling, A. Poljak, R. Grant, Age related changes in NAD+ metabolism oxidative stress and Sirt1 activity in wistar rats, *PLoS One*. 6 (4) (2011) e19194, https://doi.org/10.1371/journal.pone.0019194.

[22] D. Tafrali, Post-Mortem Changes and Autolysis in Frontal Lobe Cells of Sus Scrofa - A Cellular And Subcellular Ultrastructural Analysis Via Transmission Electron Microscopy, Medical University of Graz, Graz – Austria, 2019. MD Thesis.

[23] H. Anderton, S. Alqudah, Cell death in skin function, inflammation, and disease, *Biochem. J* 479 (15) (2022) 1621–1651, https://doi.org/10.1042/BCJ20210606.